iJRASET
International Journal For Research in Applied Science and Engineering Technology

INTERNATIONAL JOURNAL FOR RESEARCH

IN APPLIED SCIENCE & ENGINEERING TECHNOLOGY

Volume: 6 **Issue:** III **Month of publication:** March 2018

DOI: http://doi.org/10.22214/ijraset.2018.3728

www.ijraset.com

Call: 08813907089 | E-mail ID: ijraset@gmail.com

International Journal for Research in Applied Science & Engineering Technology (IJRASET)
ISSN: 2321-9653; IC Value: 45.98; SJ Impact Factor: 6.887
Volume 6 Issue III, March 2018- Available at www.ijraset.com

Pore Pressure Prediction of Concrete Exposed to Fire

A.Arul Peter[1], K. Murugesan[2],Umesh Kumar Sharma[3]
[1]*Assistant Professor, Vels University, Pallavaram, Chennai,*
[2]*Associate Professor Mechanical & Industrial Engineering Department, IIT Roorkee, Roorkee,*
[3]*Associate Professor, Department of Civil Engineering, IIT Roorkee, Roorkee, India*

Highlights

A. Concrete column exposed to ISO 834 fire is modeled.
B. This model predicts temperature, moisture and pore pressure profiles.
C. Remarkable peak pore pressure is observed at 5 minutes.
D. Up to 12 minutes, the pore pressure wave front over take the vapor front.

Abstract: ***This paper deals with concrete exposed to ISO 834 fire. Mathematical model is developed from conservation of energy, mass for air and liquid and water vapor. The evaporation and condensation of water increases pore pressure inside the concrete is studied and discussed. Up to 12 minutes, the pore pressure wave front over take the vapor front. However, at the end of 25 minutes the situation get reversed due to increase in porosity of concrete at high temperatures. The effect of thermal conductivity and other transport properties on temperature and pore pressure histories are also analyzed.***
Key words: coupled heat and mass transfer, unsaturated porous material, concrete, initial transient, temperature, pore pressure

I. INTRODUCTION

The study of the performance of concrete exposed to high temperatures and fire find wide engineering applications such as protection of nuclear reactors from accidental fire, high rise buildings etc. These events and recent research work have highlighted the lack of complete understanding of how concrete behaves under rapid thermal loading. For controlling the disintegration and the degradation of the material before attaining elevated temperatures, it is essential to understand the heat and mass transport mechanisms inside concrete. This can be achieved either by conducting experimental trials or through simulation work. Though experimental works provide valuable data and information on the failure of concrete exposed to elevated temperatures, it is not possible to understand the physics behind all the transport phenomena due to the multi-scale, non-linear and coupled transport processes that take place inside a concrete. Hence numerical simulation is considered as one of the efficient tools to study the heat and moisture transport within concrete. However, these simulation results also need to be validated with experimental data to make it more reliable for predictions.

Jean Christophe et al.[1] constructed an experimental set up to measure pore pressure build up within concrete for five different water cement ratios and concluded that compactness of concrete created high pore pressure. They considered only the transport properties such as, porosity, permeability and water content as parameters for their study. Kalifa et al. [2] designed experimental set up in which one of the faces of concrete was heated upto 800°C. Their experimental research concluded that high pore pressure buildup was observed in concrete of low porosity. The mechanism behind the mass transport in porous media was well understood from volume_averaging equations from formal theory of drying without considering dehydration starting from point equations in each phase [3]. Bazant et al.[4] developed semi empirical relations for sorption isotherms as a function of permeability, temperature and change of porosity due to dehydration from experimental data upto critical temperature of water. They represented the transition region using a linear relation between saturated and unsaturated regions. Though their model has been widely used in numerical simulations, often instability and computational difficulty were faced from this model due to the inflection points at the two limits of the regions. Majumdar et al. [5] proposed a S-shaped smoother transition region to overcome the computational difficulties and instabilities. Ahmed et al. [6] presented a model for thermal response of concrete subjected to ASTM E119 and ASTM E1529 fire curves. Their model predicted the coupled heat and mass transfer in concrete as porous media based on mass, momentum and energy conservation principles. The model was validated against temperature data obtained from experiments maintaining consistency among three coupled output parameters, temperature, moisture content and pore pressure. Gawin et al.[7] developed a non-linear hygro-thermal model which predicted the behavior of concrete structures subjected to thermal loads in the

presence of multiphase flow and phase change below the critical point of water. They concluded that capillary pressure has no effect above the critical point and only physically adsorbed water was considered at a particular state. Newton type numerical technique was employed to solve the non-linear equations which yield the capillary pressure, gas pressure, temperature as output parameters. Tenchev et al.[8] developed a coupled heat and mass transfer model from several physical quantities and used semi analytical relations for the prediction of pore pressure. Direct iterative numerical procedure was adapted to predict the output temperature, pore pressure and vapor content per unit volume. Davie et al. [9] confirmed the observations made by Gawin et al. [7] for the behavior of capillary water and adsorbed water above the critical point. In their model they assumed that the relative permeability of water was not 100% and it depended on the saturation level of concrete. Dwaikat et al. [10] insisted that the influence of relative humidity on pore pressure build up leads to spalling. Their model was validated and analyzed the concrete under the exposure of ASTM E119 standard fire curve. They concluded that low value of relative humidity also causes sufficiently large pore pressure build up due to the dehydration of non-evaporable water that is chemically bound with cement paste which was dehydrated. A three-dimensional numerical model was proposed to investigate the roles of various mechanical behaviors in the overall hygro-thermo-mechaical response of ordinary and high performance concrete by Davie et al.[11].

the present research paper an attempt is made for a detailed study on the evolution of initial transients of temperature and pore pressure variation for a concrete exposed to fire. The main focus of the work is to highlight the interaction effects on the initial transients of vapor generated due to the heavy thermal load, with the material properties of concrete and other transport properties. For this purpose a mathematical model based on conservation equations are developed and solved using finite element method. The problem of concrete exposed to fire involves processes that lead to destruction of the solid after around 40 minutes to one hour. It is the initial transients that control all the later physical phenomena that weaken the material. Hence, simulation results are obtained for the initial 30 minutes duration of exposure of concrete to fire. Results obtained are illustrated as time and spatial variations of the field variables as well as the variation of important transport properties with temperature. The details of mathematical formulation, numerical procedure and discussion on the simulation results are given in the following sections.

II. PROBLEM DESCRIPTION

A two dimensional rectangular cross section of concrete column exposed to fire is considered as the computational domain as shown in Figure 1. The specimen is symmetrical about the x- axis so that the computed temperature, pore pressure and vapor content are symmetrical about this horizontal axis. The left side of the concrete specimen is assumed to be exposed to fire, whereas the top and bottom sides are assumed to be adiabatic and the right side is left as free boundary condition. The computational mesh comprises of one element in vertical direction and variable number of elements in horizontal direction of length 0.1m. The computational domain is discretized using four node quadrilateral square elements. Numerical simulation will focus on the computation of temperature, pore pressure and vapor content at every node of the domain at different time intervals.

A. Governing Equations

Concrete can be treated as a multiphase porous media comprising of solid, liquid and gaseous phases (water vapor and air). Hence representative elementary volume (REV) approach as proposed by Whitaker et al. [3] had been employed for modeling heat and moisture transport through the concrete. The multi-phase transport phenomenon in a concrete is modeled using energy conservation, moisture conservation and air conservation equations. The derived equations based on Whitaker's theory of drying (volume averaging method) for energy, liquid water and vapor and air conservation are modified as given below [8]:

Energy equation

$$(\rho C)\frac{\partial T}{\partial t} = -\nabla.(k\nabla T) - (\rho C v)\nabla T - \lambda_E E_L - \lambda_D \frac{\partial \bar{\rho}_D}{\partial t} \quad (1)$$

Moisture conservation equation

Liquid water conservation

Rate of change of liquid water in unit volume of concrete

$$\frac{\partial \bar{\rho}_L}{\partial t} = -\nabla.J_L + E_L + \frac{\partial \bar{\rho}_D}{\partial t} \quad (2)$$

Water vapor conservation

$$\frac{\partial(\varepsilon_G \bar{\rho}_V)}{\partial t} == -\nabla.J_V - E_L \quad (3)$$

Summing up Eqns. (2) and (3), we get

$$\frac{\partial(\varepsilon_G \bar{\rho}_V)}{\partial t} + \frac{\partial \bar{\rho}_L}{\partial t} = -\nabla.(J_L + J_V) + \frac{\partial \bar{\rho}_D}{\partial t} \quad (4)$$

Air conservation equation

$$\frac{\partial(\varepsilon_G \tilde{\rho}_A)}{\partial t} = -\nabla . J_A \quad (5)$$

The conservation equations (1), (4) and (5) are the final governing equations to be solved for the field variables, temperature (T), gas pressure (P_G) and vapor content ($\tilde{\rho}_V$). As these equations are coupled and non-linear finite element method is employed to solve the equations.

B. Initial and Boundary conditions

The initial conditions: At $t = 0$ the field variables are

$$T^0 = 20℃; P_G^0 = P_{G\infty} = 0.1\, MPa; \rho_L^0 = 60\, kg/m^3; \emptyset = 0.8$$

$$P_V^0 = P_{Sat}^0(T^0)\tilde{\rho}_V^0 = P_V^0/(T^0 R_V) \quad \tilde{\rho}_{V\infty}^0 = \tilde{\rho}_V^0 \emptyset$$

The left side of the domain is assumed to be subjected to convective heat and mass transfer boundary conditions, the top and bottom surfaces are treated as adiabatic whereas the right side is left as free boundary condition.

Conservation of energy

$$k\frac{\partial T}{\partial n} + h_{qr}(T - T_\infty) = 0 \quad (6)$$

Water vapor boundary condition

$$J_V . n - \beta(\tilde{\rho}_v - \tilde{\rho}_{v\infty}) = 0 \quad (7)$$

Pressure boundary conditions

The pressure on the boundary surface was assumed to be equal to atmospheric pressure

$$P_G^0 = P_{G\infty} \quad (8)$$

C. Finite Element Formulation

Heat and moisture transport through concrete exposed to fire is initiated by the external heat load due to fire. Diffusion of heat causes the solid temperature to rise and evaporate the water used while mixing with other materials. Water evaporated tries to move through the concrete, whenever it does not find enough space to move through, then it got stagnant resulting in pore pressure build up. The moisture present inside an unsaturated porous media depends upon the material sorption characteristics, which in turn is a function of temperature, vapor content and vapor pressure. Hence it may be concluded that temperature, pore pressure and vapor are all coupled to each other. Unless the governing equations (1), (4) and (5) are rewritten in terms of temperature, pore pressure and water vapor as coupled equations, the physical phenomena that took place inside concrete cannot be correctly predicted. For this purpose the above equations are manipulated to obtain the following equations after relating the relevant properties with the field variables. The details of the derivations can be obtained from Ref [8]

.

$$C_{TT}\frac{\partial T}{\partial t} + C_{TP}\frac{\partial P_G}{\partial t} + C_{TV}\frac{\partial \tilde{\rho}_V}{\partial t} = \nabla.(K_{TT}\nabla T + K_{TP}\nabla P_G + K_{TV}\nabla\tilde{\rho}_V) \quad (9)$$

$$C_{MT}\frac{\partial T}{\partial t} + C_{MP}\frac{\partial P_G}{\partial t} + C_{MV}\frac{\partial \tilde{\rho}_V}{\partial t} = \nabla.(K_{MT}\nabla T + K_{MP}\nabla P_G + K_{MV}\nabla\tilde{\rho}_V) \quad (10)$$

$$C_{AT}\frac{\partial T}{\partial t} + C_{AP}\frac{\partial P_G}{\partial t} + C_{AV}\frac{\partial \tilde{\rho}_V}{\partial t} = \nabla.(K_{AT}\nabla T + K_{AP}\nabla P_G + K_{AV}\nabla\tilde{\rho}_V) \quad (11)$$

Now equations (9) to (11) are the final governing equations that has to be solved as coupled equations. It has to be observed that all the coefficient matrices in the above equations are also functions of the field variables. Hence the non-linear coupled governing equations are solved using Galerkin's weighted residual finite element method through an iterative solution algorithm. The finite element procedure is based on a piecewise approximation of the unknown vector using a shape function. Galerkin's weighted residual method is widely used for the solution of field equations and it is based on the principle of minimization of residue obtained as a result of the assumed approximate solution for the given equation. Any generalized transient equation can be represented using Galerkin's method as

$$\sum\int\int N^T[C]_{ij}\, N dxdy = -\sum\int\int \nabla N^T[K]_{ij}\,\nabla N dxdy \quad (12)$$

where N is the shape function selected for the type of element chosen for discretizing the computational domain. In the present research 4-node quadrilateral elements are used to discretize the computational domain. Isoparametric formulation has been employed to represent the quadrilateral elements as it allows integration of matrices using Gaussian quadrature. Computational mesh is generated using transfinite interpolation (TFI) method.

Gauss iterative solver is employed for the solution of the final nodal equations. The solution field for temperature, pore pressure, and mass per unit volume of vapor content is assumed to be converged for the time step 'i' when the error between two consecutive iterations 'j' and '$j+1$' for any primary variable is satisfied as follows: $\Delta_j^i \Lambda = \frac{\sum_{k=1}^{nnodes}\left((\Lambda_k)_{j-1}^i - (\Lambda_k)_j^i\right)^2}{\sum_{k=1}^{nnodes}\left((\Lambda_k)_j^i\right)^2} < 10^{-9}$ where '*nnode*' is the total number of grid points in the computational domain.

III. RESULTS AND DISCUSSION

A. *Validation Results*

The model and the computer code developed for the simulation of heat and moisture transport inside concrete exposed to fire is initially validated with results available in the literature. For this purpose the concrete problem considered by Tenchev et al. [8] has been selected for comparison of the present results. A high performance concrete is assumed to be exposed to a fire simulated by ISO 834 fire curve. The schematic diagram of the concrete is shown in Figure 1 with the boundary conditions. Using a computational mesh of 50 elements with 101 nodes the temperature variation with distance along the x-axis of the concrete at the end of 30 minutes are obtained. Figure 2 shows the comparison of temperature results with the experimental and numerical results given by Tenchev et al. [8]. The solid line represents the present results, which are in close agreement with the simulation results of Tenchev et al. [8]. Close agreement with the experimental results are observed at both the ends of the concrete, whereas a slight deviation is observed in the region closer to one-fourth of the length of the concrete. It is interesting to note that a similar deviation is also observed by Tenchev et al. [8] as illustrated in the above figure. After validating the code, simulation results are obtained to understand the initial transients, the details of which are discussed in the following sections.

B. *Temperature Transients*

For the purpose of simulation, the material property data as given by Tenchev et al. [8] have been used. The sorption isotherm given by Bazant et al. [2] has been employed using smoothening as suggested by Majumdar et al. [5]. The volume fraction of free water content in the concrete below critical temperature (374.15 ℃) was estimated from sorption isotherms defined by Bazant et al.[2]. A smoothed transition between unsaturated and saturated was achieved to avoid numerical instability. All the details of derivation and expressions for different transport properties were omitted in this paper as they can be obtained elsewhere [8]. Whatever mathematical formulations used to describe the physical phenomena inside concrete exposed to fire were based on continuum principle, which yield balance equations. However, the concrete exposed to fire will be completely destroyed, say after one hour or so. In such situations it may be difficult to model all the physical destruction of the materials, though to some extent the mechanical structural failure of the concrete may be formulated. It should be noted that as the concrete exposed to fire is a strong time dependent problem, the initial transients are the determining phenomena that control the consequent physical processes. Hence in the present research, simulation results are obtained for the variation of temperature, pore pressure and water vapor at different time intervals starting from1 minute up to 30 minutes so that the actual transport phenomena that gives rise to high pore pressure can be understood.

When the concrete is exposed to fire heat is transferred by conduction and the conducted energy is transported to the fluids present in the pore structure. By convection the heat is transmitted to the water and air present in the pores. The total heat transported into the concrete is used for the following: to heat the solid, liquid and gaseous medium present in the pores, to induce the movement of liquid water and air and to evaporate freewater into vapor. The movement of moisture through concrete contributes heat transfer and affects the temperature gradient as well as the pressure gradient. Poor thermal conductivity of concrete at elevated temperatures induces steep gradients inside concrete. At regions wherever the temperature is less than the saturation temperature of water vapor at the given pressure, condensation of water vapor takes place, thus creating a wet region. As the condensate blocks the pores for the passage of water vapor, the pore pressure suddenly increases separating the layers of concrete. Figure 3 shows the temperature distribution along the length of concrete at different time levels. After the exposure of concrete to the fire, with increase in time, the temperature gradients at the exposed surface gets intensified as depicted in the above figure. A steep jump in temperature gradient is observed especially after 10 minutes and this can be attributed to the fact that concrete is a poor conductor of heat and the temperature due to fire increases exponentially with time and hence all the heat load could not be transported into the concrete with lapse of time. The present simulation could predict the expected smooth variation of temperature along the length of the solid. Figure 4 depicts the variation of temperature with time at different depths of concrete from the exposed surface. In this figure, the steep temperature gradients were noticed only closer to the exposed surface as also observed from Figure 3. With increase in

distance, the temperature gradient decreases. Wide temperature variation is also observed only closer to the exposed surface. One can easily notice that between distances 10 mm, 20 mm, 30 mm and 40 mm, the temperature variation is noted to be very high compared to other regions of concrete. This is because, the total thermal load initially affects only the region closer to the exposed surface.

C. Vapor Transients

The total heat load from the fire is not able to penetrate the concrete completely for diffusion due to its poor thermal conductivity, hence, part of the heat is used to evaporate the water present in the concrete as free water. Vapor generation is the most critical physical phenomenon in concrete exposed to fire, because only after vapor generation, the other important physical variations get initiated. The rate of liquid variation within the concrete plays a major role in controlling all the transport phenomena, though heat load from fire is the starting point. From the energy equation (1), we can find out that the terms representing the free water and bound water released by dehydration act as sink terms, which absorb heat from the solid. As the solid gets heated up, these water try to get evaporated whenever the favorable conditions prevail inside the concrete. These conditions are determined by the structural characteristic of concrete, which is determined by the variation of porosity of concrete with temperature and the sorption isotherms of moisture present inside the pores. The amount of water evaporated depends on the relative humidity inside the pores, which in turn depends on the temperature and pressure of vapor present inside the pores. Thus these parameters make the phenomena as coupled with temperature, pore pressure and vapor content. One should understand that the problem of concrete exposed to fire is a highly transient problem that is why implicit numerical scheme was implemented for simulation. All the variations of transport and other properties of concrete with time and space contribute the main transport phenomena and only the load is determined by the field variables at the previous time level. The most essential part of solution of such problems lie in the fact that all the field variables have to be determined accurately at the first time level itself, otherwise the solution may not converge, because, whatever the field variable determined at a given time level will produce the load against which the field variables at the next time level need to be computed. Hence prediction of correct field variables at the very beginning of time cycle becomes very determining in such problems.

Figure 5 shows the variation of water vapor generated along the length of concrete at different time intervals. It can be observed that with increase in time after 5 minutes, the peak of vapor generation keeps moving inside the concrete. Compared to the value at 5 minutes, the vapor generated has become more than three times at 10 minutes. Beyond 10 minutes, though there was a continuous increase in vapor generation, the rate at which vapor is being generated decreases and this becomes more significant beyond 20 minutes, and almost remains constant at about 21.5 kg/m^3 between 25 and 30 minutes. As the distance from the exposed surface increases, the amount of vapor generated shows a decreasing trend as observed in Figure 6. It is easily observed from this figure that the maximum vapor generation takes place only at 10 mm, 20 mm and 30 mm distances from the exposed surface. This is on the expected line of underlying physics because the temperature is observed to be very steep only at regions closer to the exposed surface. The heat load from the fire can be transported both by diffusion and convection by the liquid, vapor and gaseous phases, however, the main contribution comes only from diffusion.

D. Pressure Transients

The vapor thus generated by the heat load from the fire should get diffused through the concrete and convected through concrete pores. The pores were small and hence all the huge amount of vapor generated cannot pass through the pores. It should also be noted that the vapor generation is due to the high temperature gradient at the surface, hence the vapor generation is not a smooth and gradual one, but it takes place in a short duration of time. Thus the vapor generated does not find enough space and time to move within the concrete, at the same time, the temperature gradient closer to the surface keeps increasing with time, multiplying the vapor generation phenomena without any control. The temperature variation due to fire was exponential in time and hence the vapor generation also takes place expeditiously. This results in an unbalance between the vapor generated and the vapor transported within the concrete at a given distance at a given time. Hence the extra vapor that could not be transported at a faster rate within the concrete simply gets accumulated at a given location and this results in pore pressure rise. Figure 7 shows the pressure distribution within the concrete at different time intervals. These figures indicate that initially the pressure increases, reaches a maximum value and then start decreasing. In the simulation it was assumed that initially the gaseous phase in the concrete was at 100 kPa. Hence this initial value is shown as 0 in the pressure scale in the above figure. As observed in Figure 5 for vapor distribution, here also there is an increase of more than three times in pressure from 5 minutes to 10 minutes. The pressure is always steep all the time, however, the rate of increase of peak pressure decreases after 10 minutes as also observed in Figure 5 for vapor distribution. The

pore pressure reached a maximum value of about 5.2 MPa at 30 minutes. This is on the expected physics behind the problem because the peak pressure rise takes place only because of accumulation of excess vapor that could not be transported through the concrete. Figure 8 shows the pressure variation with time at different depths of concrete. These plots also confirm the phenomena predicted by vapor distributions that the maximum vapor generation and hence the consequent pressure rise takes place only up to a distance of 30 mm from the exposed surface of the concrete.

E. Influence of Transport Properties

The peak pore pressure takes place only because of the excess vapor accumulated inside the concrete. Though pressure variation is coupled with vapor generation, it was not clear how these two fronts will move within the concrete. For this purpose, the peak pressure and vapor variations along the distance of concrete at different time levels had been computed and plotted as shown in Figure 9. It can be seen from this figure, that up to the initial 15 minutes, the pore pressure takes a lead to travel inside the concrete leaving the vapor peak to follow. Surprisingly both the fronts travel at the same speed from 15 minutes to about 25 minutes and beyond this, the vapor front took over the pore pressure front. Initially the vapor front lags behind the pressure wave because the porosity is not high enough to allow the easy passage of vapor to travel inside the concrete. With increase in time, the temperature of solid increases due to high temperature gradients near the exposed surface, thus favoring immense free water evaporation. In addition to this, with increase in temperature, the porosity of concrete also increases, thus the water vapor transport increases. This results in a situation where both the pore pressure and vapor fronts travel at the same speed. However, at about 25 minutes, the increase in porosity is sufficiently high so that the vapor can easily flow through the concrete. In order to understand the effect of temperature on various transport properties during the initial transients, plots are made for the variation of porosity, thermal conductivity of concrete etc. Figure 10 shows the variation of porosity with distance at different time intervals. There is a continuous increase in porosity at regions closer to the exposed surface with time because of increase in temperature and these variations are found to vary steeply with time. The enlargement of pores also influence the easy travel of vapor at regions closer to the exposed surface. Thermal conductivity variation with distance of concrete at different time levels were depicted in Figure 11. The thermal conductivity decreases with increase in time or temperature as seen from the above figure and they vary significantly only at the regions closer to the exposed surface where steep temperature gradients are generated due to fire. Figure 12 illustrates the variation of dehydrated water released from the concrete with distance at different time intervals. There is no dehydrated water that come out of concrete up to 5 minutes, only beyond 5 minutes, this water start releasing from the concrete and its quantity increases with time, with maximum being observed at the surface and decreases drastically from the surface towards the interior of the concrete.

IV. CONCLUSION

A numerical model based on conservation equations for energy, moisture and air transport inside a concrete has been developed to understand the heat and moisture transport when concrete is exposed to high temperature such as fire. After validating the model, simulation results have been obtained for initial transients of temperature, moisture and pore pressure evolutions up to 30 minutes of exposure of concrete to fire defined by an ISO 834 fire curve. The effect of transport properties on the above field variables have also been analyzed. Based on the discussion of the above results, the following conclusions have been arrived at:

A. The poor thermal conductivity of concrete at elevated temperatures blocks heat.
B. Steep temperature gradients observed about 10 minutes of exposure.
C. This leads to condensation of water vapor.
D. Blockage of vapor starts due to inability of concrete to transport all the vapor.
E. This blockage results in increase in pore pressure.
F. The first noticeable peak pore occurs at about 5 minutes.
G. This peak keeps moving towards the interior of the concrete.
H. At 30 minutes, this peak pressure has crossed ¼ th concrete from the surface.
I. The peak pressure front moves ahead of the peak vapor front up to 15 minutes.
J. The vapor front over takes the pore pressure front after 25 minutes.
K. Porosity was increased near the peak temperature gradients closer to the fire.
L. Thermal conductivity of concrete keep on decreasing.
M. Porosity of concrete affects the transport of vapor inside the concrete.

N. Dehydration took after 5 minutes of exposure.

Ci specific heat of phase i, [J/kg^{o}C], i = A,V, S,L
D_{AV} Diffusion coefficient of air or water vapour in gaseous mixture[m^2/s]
E_L Rate of evaporation of liquid water per unit volume of concrete [kg/(m^{3}s)]
hq convective heat transfer coefficient [J/(m^{2}s ^{o}K)]
hqr h_q+h_r
J_i mass flux of phase i,per unit area of concrete [kg/(m^{2}s)], i= A,V, L
k Thermal conductivity of concrete[J/(m^{2}s ^{o}C/m)]
K Specific (intrinsic) Permeability of concrete dry concrete[m^2]
K_i relative permeability of phase i, through dry concrete[%]
P_i partial pressure of phase i, i = A,V; pressure of phase i=G,L [Pa]
P_{Sat} saturation pressure of water vapour[Pa]
p_{or}^0 initial porosity
p_{or}^* increase of porosity with temperature
R_i gas constant for phase i, i = A,V;
T temperature [^{o}C] or [^{o}K]
ε_i volume fraction of phase i[%],i=G,L,S; $\varepsilon_i = \frac{V_I}{V}$(Volumes)
λ_D specific heat of dehydration of bound water[J/kg]
λ_E specific heat of evaporation[J/kg]
β watervapour coefficient on boundary[m/s]
μ_i (dynamic) viscosity of phase i[kg/(ms)], i= A,V, G,L
ρ_i density of phase i, i=L,S
$\tilde{\rho}_i$ mass of phase i per unit volume of gaseousmixture[kg/m^3], i = A,V
$\bar{\rho}_i$ mass of phase i per unit volume of concrete [kg/m^3], i = L,D
$\bar{\rho}_{Cem}$ mass of anhydrous cement per unit volume of concrete[kg/m^3]=300kg/m^3
ρC effective heat capacity of concrete[J/ m^3 ^{o}C]
ρC_V vector of energy transport by fluid flow[J/ m^2 ^{o}C]
$\emptyset$ relative humidity of concrete
$\bar{}$ variable defined per unit volume of concrete
$\sim$ variable defined per unit volume of gaseous mixture

Subscripts
A dry air within the gaseous mixture
D released bound water by dehydration
G gaseous phase (mixture of air and water vapor)
L Liquid water phase
S dry skeleton
V water vapor
∞ Surrounding environment

Superscripts
e element number
n number of time step (n=0 initial ambient state)

ISSN: 2321-9653; IC Value: 45.98; SJ Impact Factor: 6.887
Volume 6 Issue III, March 2018- Available at www.ijraset.com

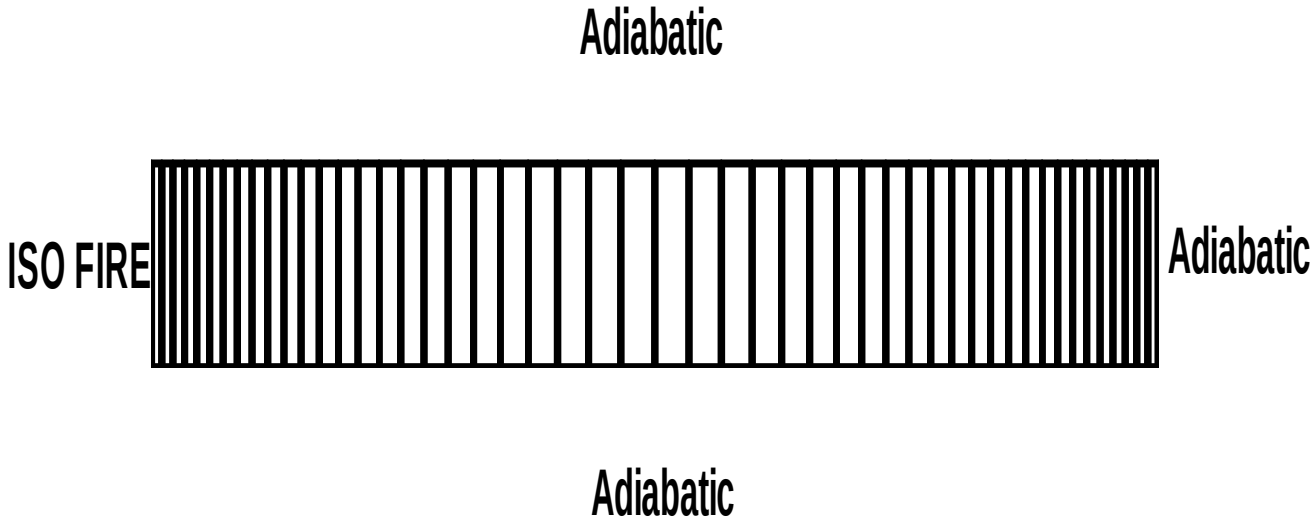

Figure 1 Schematic diagram of concrete exposed to fire

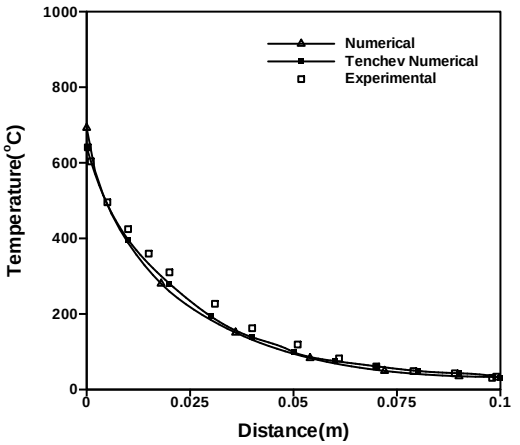

Figure 2 Temperature distribution at the end of 30 minutes

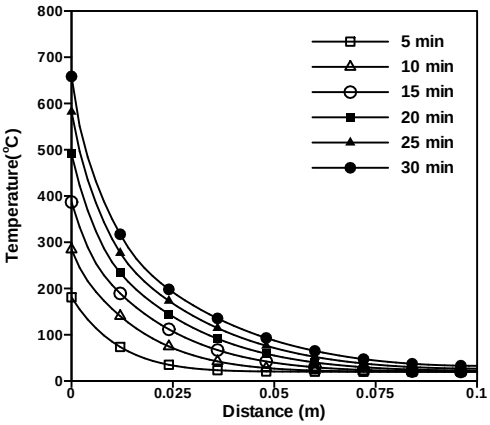

Figure 3 Distance Vs. Temperature

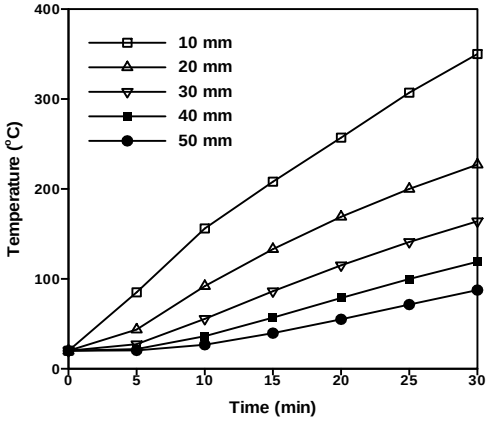

Figure 4 Time Vs. Temperature

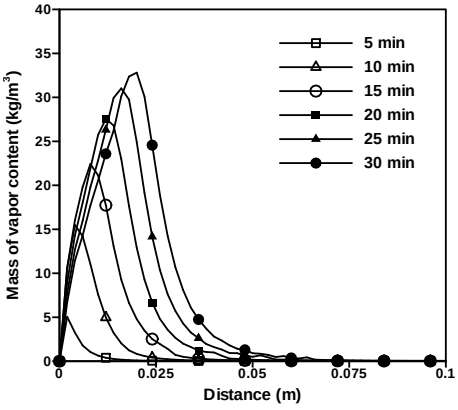

Figure 5 Distance Vs. mass of water vapor per unit volume

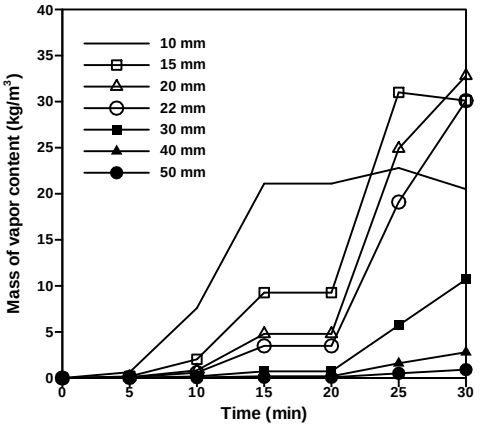

Figure 6 Time Vs mass of water vapor per unit volume

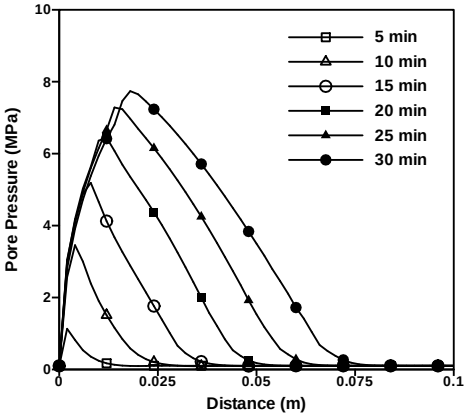

Figure 7 Distance Vs pore pressure

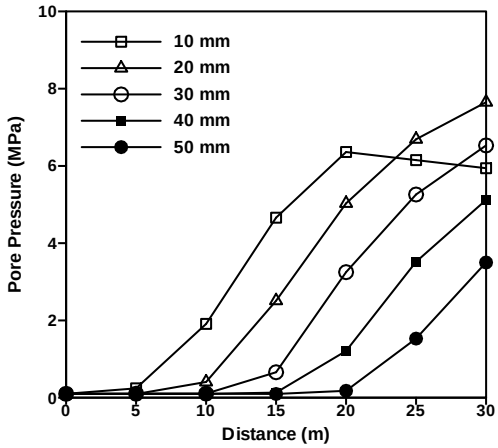

Figure 8 Time Vs pore pressure

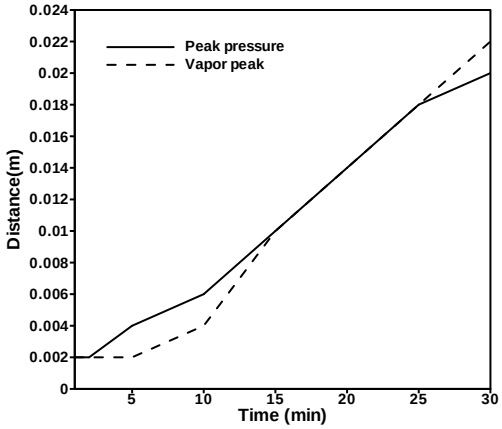

Figure 9 Movement of pore pressure and water vapor fronts

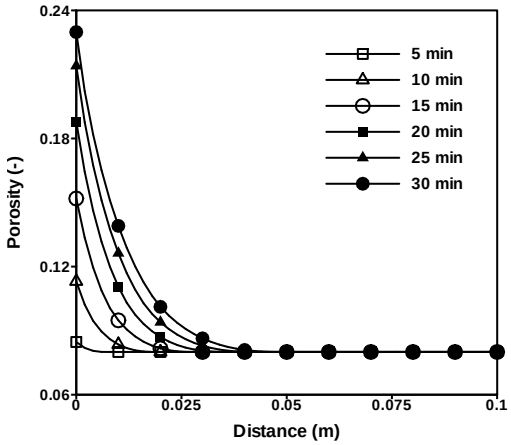

Figure 10 Distance Vs porosity

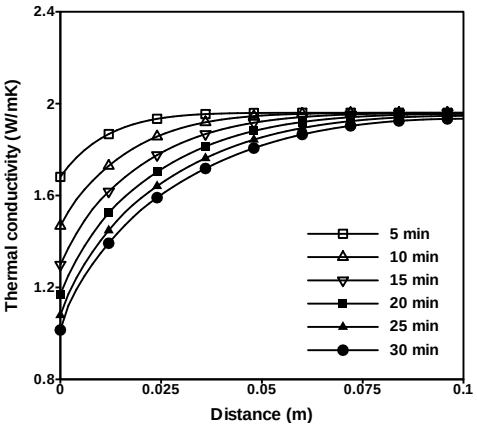

Figure 11 Distance Vs Thermal conductivity

$$p_{or} = {}^{0}p_{or} \times \begin{cases} 1 & \text{for } T < 100^{\circ}C \\ aT^3 + bT^2 + cT + d & \text{for } 100^{\circ}C < T \le 800^{\circ}C \\ 3 & \text{for } T > 800^{\circ}C \end{cases}$$

$$k_{eff} = 2 - 0.24\left(\frac{T}{120}\right) + 0.012\left(\frac{T}{120}\right)^2$$

where ${}^{0}p_{or} = 0.08, a = 1.095238e-8, b = 1.471428e-08,$ $c = -2.3904762$ and $d = 1.1028571$

where ${}^{0}p_{or} = 0.08, a = 1.095238e-8, b = 1.471428e-08,$ $c = -2.3904762$ and $d = 1.1028571$

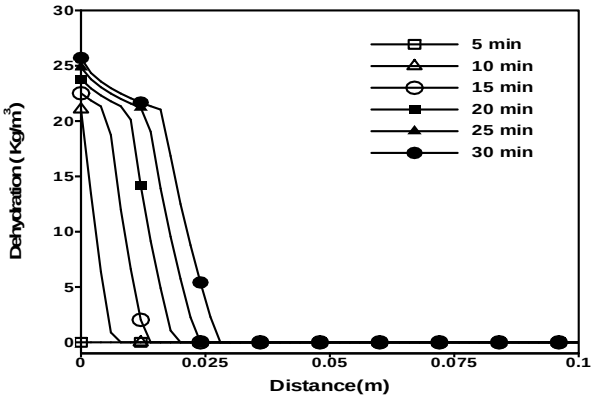

Figure 12 Distance Vs dehydration

$$\bar{\rho}_D = \bar{\rho}_{Cem} \times \begin{cases} 0 & if\ T \leq 200℃ \\ 7.0 \times 10^{-4}(T - 200) & if\ 200℃ > T \leq 300℃ \\ 0.4 \times 10^{-4}(T - 300) + 0.07 & if\ 300℃ > T \leq 800℃ \\ 0.09 & if\ T > 800℃ \end{cases}$$

REFERENCES

[1]. Jean-Christophe Mindeguia, Pierre Pimienta, Albert Noumowe, Muluba Kanema, 2010, "Temperature, pore pressure and mass variation subjected to high temperature-Experimental and numerical discussion on spalling risk", cement and concrete research 40, pp477-487. doi.org/10.1016/j.cemconres.2009.10.011

[2]. Pierre Kalifa, FrancËois-Dominique Menneteau, Daniel Quenard, 2000, "Spalling and pore pressure in HPC at high temperatures", Cement and Concrete Research,30, pp1915-1927. DOI:http://dx.doi.org/10.1016/S0008-8846(00)00384-7

[3]. S.Whitaker, 1977, "Simultaneous heat, mass, momentum transfer in porous media, A theory of drying in J.P.Hartnett and T.F.Irvine (Eds.)", Advances in Heat Transfer, Academic Press, New York, 13, pp 119-203. DOI:10.1016/S0065-2717(08)70223-5

[4]. Z. P.Bazant, J. C. Chern, and W.Thonguthai, 1981, " Finite element program for moisture and heat transfer in heated concrete", Nuclear Engineering and Design, 68, pp 61-70. doi.org/10.1016/0029-5493(82)90040-1

[5]. P.Majmudar, A.Gupta, A. Marchertas, 1995, " Moisture propagation and resulting stress in heated concrete walls ", Nuclear Engineering and design, 156 pp 159-165. doi.org/10.1016/0029-5493(94)00940-Z

[6]. G. N. Ahmed, J. P. Hurst, 1999, " Modeling pore pressure, moisture, and temperature in high strength concrete columns exposed to fire", Fire Technology, 35 pp 232-262.

[7]. D.Gawin, C. Majorana, B.A. Schrefler, 1999, "Numerical analysis of hygro-thermal behaviour and damage of concrete at high temperature", Mechanics of cohesive-frictional material,4, pp 37-74. DOI:10.1002/(SICI)1099-1484(199901)4:1<37::AID-CFM58>3.0.CO;2-S

[8]. R.T.Tenchev, L.Y. Li, and J.A.Purkiss, 2001, "Finite element analysis of coupled heat and moisture transfer in concrete subjected to fire", Numerical Heat Transfer, A, 39, pp 685-710. DOI: 10.1080/10407780119853

[9]. C.T. Davie, C.J. Pearce, N.Bicanic,2006, "Coupled heat and moisture transport in concrete at elevated temperatures-effects of capillary and adsorbed water", Numerical Heat Transfer, A, 49(2006)733-763. DOI: 10.1080/10407780500503854

[10]. M. B. Dwaikat, V. K. R. Kodur, 2009, "Hydrothermal Model for predicting fire induced spalling in concrete structural systems", Fire Safety Journal, 44, pp 422-434. doi:10.1016/j.firesaf.2008.09.001

[11]. C.T.Davie, C. J. Pearce, N. Bicanic,2010, "A fully generalized, coupled, multiphase, hygro-thermo-mechanical model for concrete", Materials and structures. 43, pp 13-33. DOI 10.1617/s11527-010-9591-y

[12]. D.Gawin, F. Pesavento, B. A. Schrefler, 2002a " Modelling of hygro thermal behaviour and damage of concrete at high temperature above the critical point of water", International journal for Numerical and Analytical Methods in Geomechanics.26, pp 537-562. DOI: 10.1002/nag.211

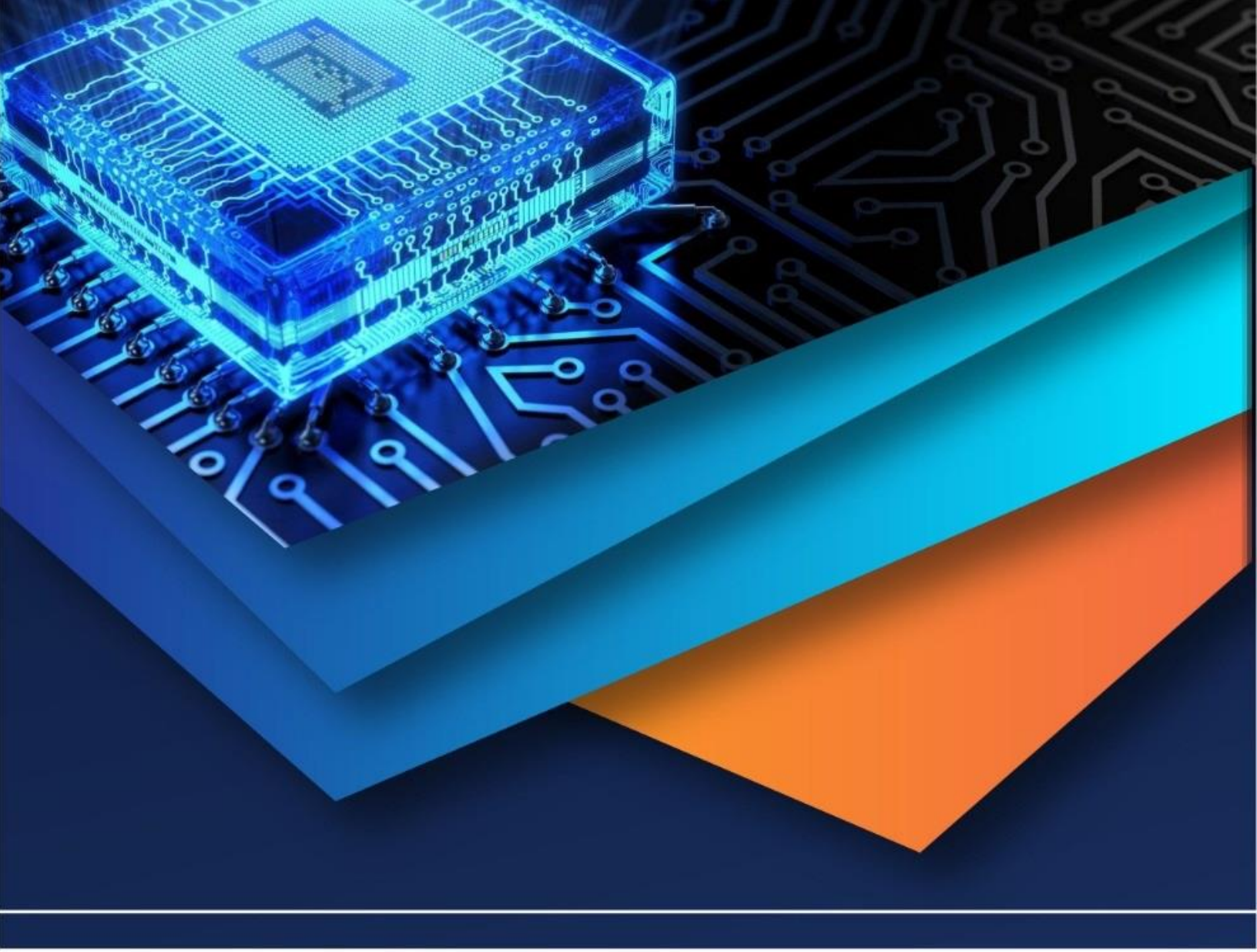

10.22214/IJRASET

45.98

IMPACT FACTOR: 7.129

IMPACT FACTOR: 7.429

INTERNATIONAL JOURNAL FOR RESEARCH

IN APPLIED SCIENCE & ENGINEERING TECHNOLOGY